REVIEW

National Science Review
1: 277–292, 2014
doi: 10.1093/nsr/nwt003
Advance access publication 7 December 2013

MATERIALS SCIENCE

Recent advances in graphene-based planar micro-supercapacitors for on-chip energy storage

Zhong-Shuai Wu[1], Xinliang Feng[1,2,*] and Hui-Ming Cheng[3,*]

ABSTRACT

The current development trend towards miniaturized portable electronic devices has significantly increased the demand for ultrathin, flexible and sustainable on-chip micro-supercapacitors that have enormous potential to complement, or even to replace, micro-batteries and electrolytic capacitors. In this regard, graphene-based micro-supercapacitors with a planar geometry are promising micro-electrochemical energy-storage devices that can take full advantage of planar configuration and unique features of graphene. This review summarizes the latest advances in on-chip graphene-based planar interdigital micro-supercapacitors, from the history of their development, representative graphene-based materials (graphene sheets, graphene quantum dots and graphene hybrids) for their manufacture, typical microfabrication strategies (photolithography techniques, electrochemical methods, laser writing, etc.), electrolyte (aqueous, organic, ionic and gel), to device configuration (symmetric and asymmetric). Finally, the perspectives and possible development directions of future graphene-based micro-supercapacitors are briefly discussed.

Keywords: graphene, supercapacitors, mirco-supercapacitors, planar, interdigital, energy storage

[1]Max Planck Institute for Polymer Research, Ackermannweg 10, 55128 Mainz, Germany, [2]School of Chemistry and Chemical Engineering, Shanghai Jiao Tong University, Shanghai 200240, China and [3]Shenyang National Laboratory for Materials Science, Institute of Metal Research, Chinese Academy of Sciences, Shenyang 110016, China

***Corresponding authors**. E-mails: cheng@ imr.ac.cn; feng@mpip-mainz.mpg.de

Received 6 September 2013; **Revised** 25 September 2013; **Accepted** 25 September 2013

INTRODUCTION

Supercapacitors (also called electrochemical capacitors or ultracapacitors) have attracted great interest in recent years because they offer a balanced energy density and power density that bridge the gap between batteries and conventional capacitors (Fig. 1) [1]. As a result, supercapacitors can be used for various high-power applications in portable electronics, electric vehicles and hybrid electric vehicles [2–5]. They also possess other desirable features, such as pollution-free operation, high charge/discharge efficiency and are maintenance-free [6].

Recently, the rapid development of miniaturized portable electronic devices, such as micro-electromechanical systems, microrobots and implantable medical devices, has greatly stimulated the need for micro-/nano-scale power sources [7]. Miniaturized micro-batteries that store energy by either redox or expansion–contraction reactions are the most dominantly used micro-power source for current portable electronics [8]. However, they have the drawbacks of limited lifetime (hundreds or thousands of cycles) and low power density that prevent applications that require high power over a short time. Alternatively, micro-supercapacitors (MSCs) are new miniaturized high-power micro-electrochemical energy-storage devices [9–13]. Their advanced features include ultrahigh power density that is several orders of magnitude larger than that of batteries and conventional supercapacitors, faster rate capability and superior cycling lifetime (millions of cycles). Therefore, MSCs are very promising miniaturized ultrahigh-power microdevices that offer sufficient peak power for numerous applications [9–13]. Currently, MSCs are mainly targeted for electronics and other on-chip uses that can be directly coupled to micro-electromechanical systems, energy harvesting micro-systems, energy-storage units, and power supplies for powering micro-sensors, electronic devices, biomedical implants, and active radio frequency identification tags [9–13]. Despite great advances in this area, the research and development of MSCs are still at a relatively early and fundamental stage. Further efforts are urgent to improve their performance and realize their practical applications.

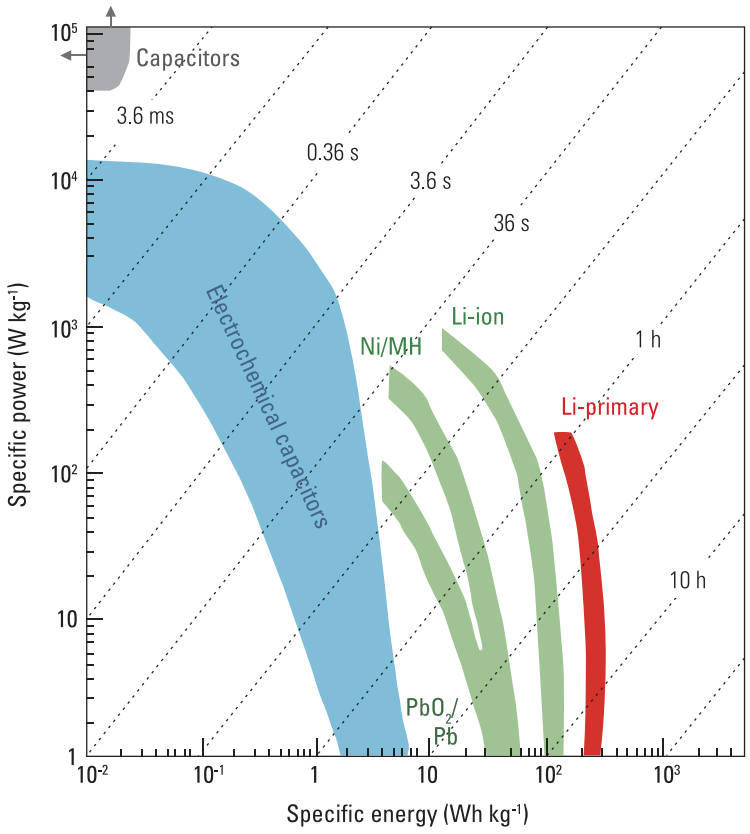

Figure 1. Ragone plot related to specific energy and power of typical electrochemical capacitors compared with other electrical energy-storage devices. Reprinted with permission from Simon and Gogotsi [1]. (Copyright 2008, Macmillan Publishers Limited.)

Supercapacitors

Traditionally, a supercapacitor is composed of two collectors, two electrodes, a separator and an electrolyte, and the cell is assembled into a sandwich-like stacked configuration of a collector/electrode/separator/electrode/collector and is surrounded with sealing and packaging materials (Fig. 2) [14]. The electrolyte mostly consists of a conductive liquid mixture of an aqueous or organic solvent that can migrate into and out of the two electrodes during the charge and discharge process. The two electrodes are mechanically separated by an ion-permeable membrane that serves as a separator between the two electrodes to prevent a short circuit. The metallic collectors electrically connects the electrodes as the input/output terminals of electricity to an outside circuit [15,16].

Depending on the charge-storage mechanism, supercapacitors are usually divided into three categories (Fig. 3) [17,18]: (1) electric double-layer capacitors (EDLCs) that electrostatically store charges on the interface of high surface area carbon electrodes, (2) pseudocapacitors that achieve electrochemical storage of electrical energy with electron transfer during reversible redox reactions, typically, based on metal oxide and conducting polymers, and (3) hybrid supercapacitors that consist of special hybrid electrodes or asymmetric electrodes that have both the significant double-layer capacitance of carbon and the pseudocapacitance of an electronically conducting polymer or transition metal oxide. In principle, EDLCs can achieve rapid charge storage but deliver relatively low capacitance, while pseudocapacitors offer high capacitance but suffer from poor rate capability and low-cycle performance. Hybrid supercapacitor systems that combine the advantageous features of EDLCs and pseudocapactiors are becoming a more attractive choice that can simultaneously achieve high-energy and power densities in one device. Nevertheless, the performance of all the above supercapacitors definitely depends on the properties of their active materials, fabrication of electrodes, selection of electrolytes and geometry of the devices [19–21].

Graphene-based supercapacitors

Undoubtedly, graphene has aroused an explosion of interest in various fields ranging from condensed matter physics to materials science, due to its unique structure and properties [22]. By far, several primary synthesis methods, including micromechanical cleavage [22], epitaxial growth [23,24], chemical exfoliation [25–29], chemical vapor deposition (CVD) [30–32], bottom-up organic synthesis [33,34], electrochemical exfoliation [35], etc., have been developed to prepare graphene materials with different qualities and in different quantities. The major possible uses of graphene in the near future include electronics [36], polymer hybrids [37], transparent conducting electrodes [38], batteries [39–41] and supercapacitors [42]. Graphene also has potential uses in sensors [43], dye-sensitized solar cells [38], field emission [44], catalysts [45], etc.

Graphene-based materials (graphene sheets and their hybrids) have been demonstrated as one class of the most promising and attractive electrode materials for supercapacitors because of their excellent conductivity, high surface area ($\sim$2620 $m^2\,g^{-1}$), exceptional intrinsic double-layer capacitance ($\sim$21 $\mu F\,cm^{-2}$) and high theoretical capacitance ($\sim$550 $F\,g^{-1}$) [46–48]. For instance, conventional supercapacitors composed of curved graphene [49], activated graphene [50], vertically oriented graphene [47], doped graphene [19], and laser-scribed graphene [48], and graphene/metal oxide hybrids [18] as bulk electrodes have demonstrated excellent performance in terms of specific capacitance and energy density. More importantly, graphene-based thin films hold great promise for

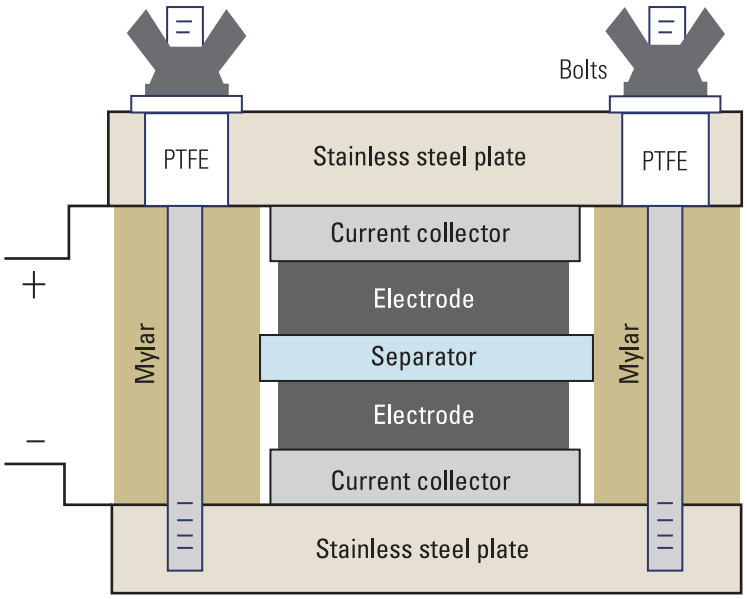

Figure 2. Schematic of the test cell configuration of supercapacitors. Reprinted with permission from Stoller *et al.* [14]. (Copyright 2008, American Chemical Society.)

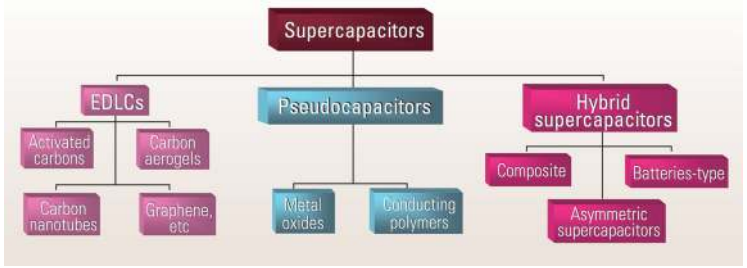

Figure 3. Typical classification of supercapacitors and related materials.

developing new types of flexible, transparent and miniaturized ultrathin supercapacitors, such as MSCs. Notably, graphene-based planar MSCs that give electrolyte ions the ability to rapidly interact with all graphene layers in the horizontal direction are superior to conventional devices [11,51].

HISTORY OF PLANAR INTERDIGITAL MSCs

With the rapid development of ultrathin, flexible miniaturized electronics, planar MSCs have attracted great attention. In comparison with conventional supercapacitors with a stack geometry, the key feature of planar MSCs is to make the entire device much thinner, smaller and flexible on an arbitrary substrate, in which electrolyte ions in the narrow interspaces between electrode fingers can be readily and rapidly transported to offer an ultrahigh power capability due to the short ion diffusion distance [9–12]. The separator commonly used in conventional supercapacitors with a stack geometry is not required in such microdevices. The different thickness of planar MSCs opens up many opportunities for the large-scale fabrication of miniaturized devices in the two-dimensional horizontal plane of a substrate for direct integration with electronics [9–12]. In contrast, the stack configuration in conventional supercapacitors is not favorable for the transport of solid or gel-type electrolytes, and this normally results in a big loss of power. In particular, the integration of conventional supercapacitors into electronics presents a big challenge that requires various processing steps to pattern the layers of current collectors, active materials and electrolyte, and to establish electrical connections at the ends [52]. Therefore, MSCs indeed have the merits of the easy fabrication of electronically isolated electrodes and integration into miniaturized electronics on the same plane, together with the broad suitability for all types of electrolytes, and the easy adjustment of electrode micropatterns, consequently leading to a decrease of internal impedance by minimizing the distance between adjacent interdigital electrodes.

From a historical viewpoint, Sung *et al.* reported the first prototype planar MSCs with a liquid electrolyte on a silicon substrate in 2003 and subsequently made a great contribution to the design and fabrication of all-solid-state and flexible MSCs [53–55]. The first example of planar MSCs is a conducting polymer interdigital MSC made by photolithography and electrochemical polymerization techniques. Typically, a metal (Au, Pt) microelectrode array was fabricated by UV photolithography and a wet-etching approach, and conducting polymers of polypyrrole (PPy) and poly-(3-phenylthiophene) (PPT) were electrochemically deposited on the microelectrodes. The obtained MSC consisted of 50 fingers (both the width of each finger and the interspace between them are ∼50 μm) and was constructed with aqueous (0.1 M H_3PO_4) and non-aqueous (0.5 M Et_4NBF_4 in acetonitrile) electrolytes. The cell potentials were between 0.6 and 1.4 V depending on the type of conducting polymers and electrolytes used [53].

Because the above devices are assembled using liquid electrolytes, one must consider the leakage of liquid electrolytes in practical applications. Therefore, developing all-solid-state MSCs that are solely made up of solid materials is required. In 2004, Sung *et al.* fabricated all-solid-state MSCs with gel-polymer electrolytes on SiO_2/Si wafers by means of wet photolithography, electrochemical polymerization and solution-casting techniques. Except for the use of a gel-polymer electrolyte, all other fabrication steps of the devices are kept almost the same. Gold microelectrodes were used

as current collectors, and PPy was used as the active material. Two kinds of gel-polymer electrolytes, an aqueous-based PVA/H_3PO_4 electrolyte and a non-aqueous-based PAN/$LiCF_3SO_3$-EC/PC electrolyte, were used. The device capacitance could be adjusted by the total amount of PPy deposited, and the working voltage was ∼0.6 V. It was concluded that the device performance of all-solid-state MSCs are comparable to that of MSCs in a liquid electrolyte [54].

To be widely applicable to flexible electronic devices, Sung *et al.* reported in 2006 the fabrication of a flexible MSC on a gel-polymer electrolyte layer substrate by photolithography, electrochemical polymerization of PPy on microelectrode arrays, followed by attaching the solidified PVA/H_3PO_4 gel-polymer electrolyte layer to the PPy microelectrode arrays and detaching the PPy microelectrode arrays from a silicon wafer [55]. The resulting device is small, lightweight and flexible, since the fabrication is from only polymeric materials. The MSC obtained can be operated at a relatively low scan rate of 100 mV s^{-1} using cyclic voltammetry (CV). No deterioration and device failure were observed even when it was bent and rolled up.

After 2006, more and more attention has been paid to developing planar MSCs by focusing on the fabrication of novel nanostructured electrode materials and the development of thin-film manufacturing techniques, such as electrochemical polymerization [55], inkjet printing [56] and layer-by-layer assembly [57], as well as the formation of new device structures from 2D to 3D microelectrodes [58–60]. Overall, the main objective is to dramatically improve the energy and power densities as well as the cycling lifetime and frequency response of the MSCs.

A series of pseudocapacitive electrode materials of metal oxide (including RuO_2 [61], MnO_2 [62], VS_2 [63]) and electrical conducting polymers (including PPy [53], PPT [53], polyaniline [64]) have been reported for MSCs. As a result, these MSCs exhibit promising volumetric stack capacitance, but suffer from low charge and discharge efficiency, frequency response and power capability. In contrast, carbon-based MSCs show a competitive and attractive potential for achieving high-frequency response and rate capability. Currently, activated carbon (AC) [59], carbide-derived carbon (CDC) [9,65], onion-like carbon (OLC) [10], carbon nanotubes (CNTs) [66] and graphene [12] have been intensively used to fabricate planar MSCs. As a typical example (Fig. 4), in 2010 Gogotsi's group developed monolithic CDC-based MSCs (CDC-MSCs) integrated with an on-chip silicon wafer by the deposition, chlorination and dry etching a TiC film into a conductive porous CDC film [9]. The CDC-MSCs showed a high volumetric capacity of 180 F cm^{-3} in tetraethylammonium tetrafluoroborate ($TEABF_4$) and ∼160 F cm^{-3} in 1 M H_2SO_4 at a low scan rate of 20 mV s^{-1}, exceeding that of all micro- and macroscale (conventional) supercapacitors so far reported, by a factor of 2. It is worth mentioning that the volumetric capacitance decreases remarkably with increasing thickness of the CDC film in both $TEABF_4$ and H_2SO_4, and is more pronounced in the organic electrolyte. For instance, a huge increase in volumetric capacitance from 30 to 180 F cm^{-3} was observed when the film thickness was reduced from 200 to 2 μm. The decrease of the capacitance with a thicker film is possibly attributed to the porosity collapse and perturbation of the interconnected structure that is crucial to facilitate electron conduction.

To achieve ultrahigh power capability and fast frequency response, Pech *et al.* developed a planar MSC by the electrophoretic deposition of a several-micrometer-thick layer of OLC with diameters of 6–7 nm on an interdigital gold current collector patterned on a silicon wafer (Fig. 5) [10]. The fabricated binder-free OLC-based MSCs (OLC-MSCs) delivered an ultrahigh power density of around 300 W cm^{-3}, comparable to an electrolytic capacitor, and showed a characteristic relaxation time constant of 26 ms that is much lower than that of an AC-based microdevice (∼700 ms) or OLC-based macroscopic device ($t > 0.1$ s). The discharge rates were measured up to 200 V s^{-1}. The combination of an interdigital microelectrode configuration, the use of a binder-free deposition technique and the nanostructured carbon onions with a high surface-to-volume ratio are responsible for the

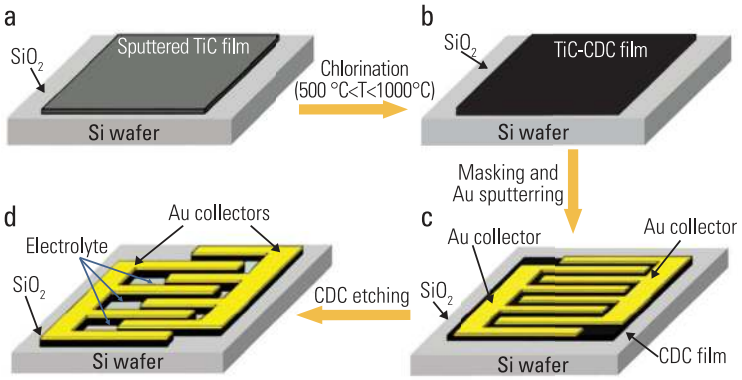

Figure 4. Schematic of the fabrication of a CDC-MSC on a silicon wafer. (a) A TiC film is deposited on a SiO_2/Si wafer by chemical and physical vapor deposition. (b) Ti is extracted from TiC as $TiCl_4$ by chlorination, forming a porous carbon film. (c, d) Standard photolithography techniques are used for fabricating CDC microelectrode arrays. Reprinted with permission from Chmiola *et al.* [9]. (Copyright 2010, the American Association for the Advancement of Science.)

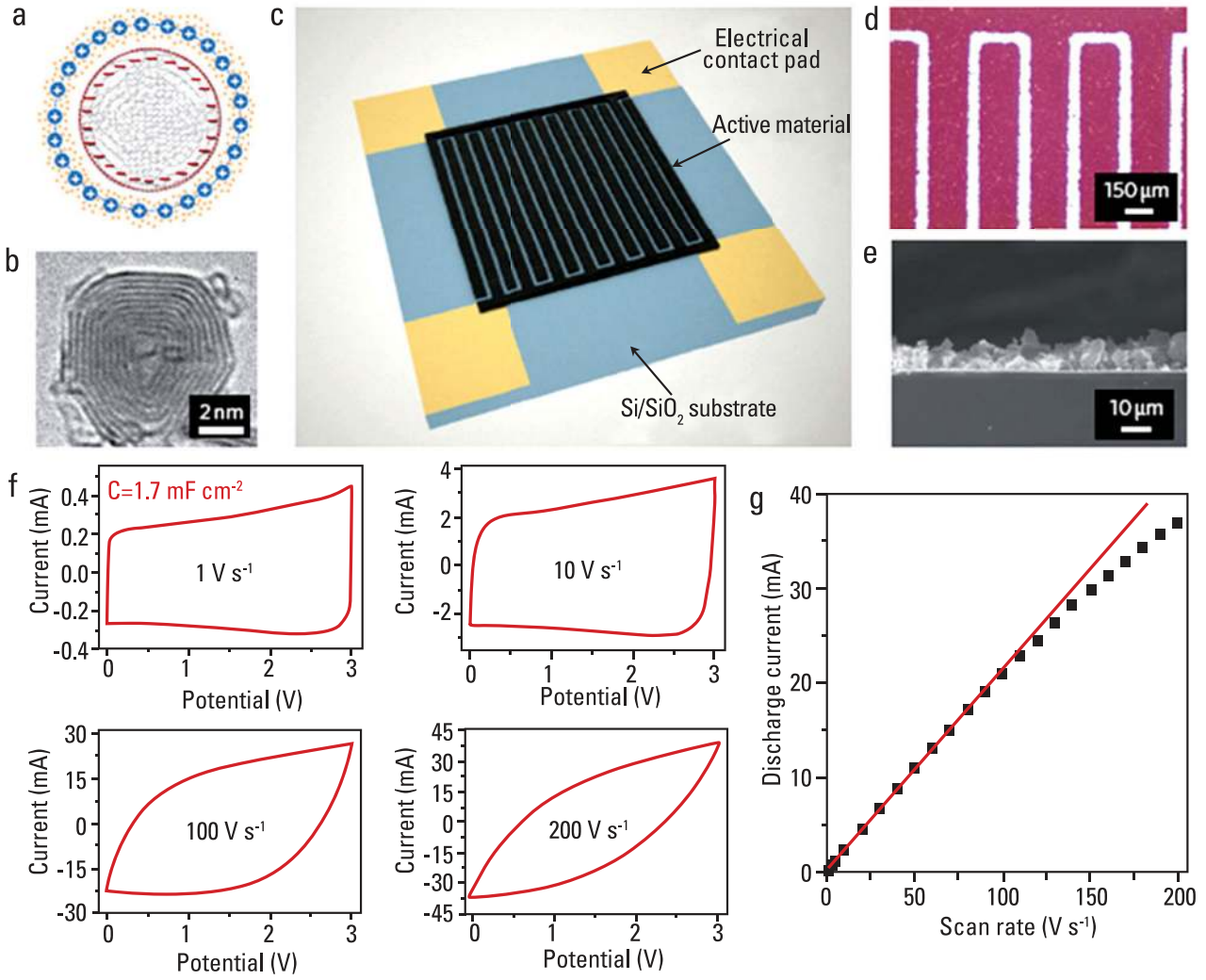

Figure 5. (a) Cross-section of a charged zero-dimensional OLC (gray) capacitor. (b) TEM image of a carbon onion. (c) Schematic of an interdigital OLC-MSC. (d) Optical image of the fingers (pink). (e) Cross-section SEM image of the carbon onion electrode. (f) CV curves obtained at different scan rates. (g) Evolution of discharge current versus scan rate. Reprinted with permission from Pech *et al.* [10]. (Copyright 2010, Macmillan Publishers Limited.)

excellent performance of the OLC-MSCs, in which the entire outer surface of the OLC is fully accessible for ion adsorption/desorption in a shorted ion diffusion pathway. The main drawback of the OLC-MSCs lies in the requirement of the high-temperature fabrication of OLC at ∼1800 °C.

Planar MSCs utilizing vertically aligned CNT forests with the design of 3D interdigital electrodes have been demonstrated by Jiang *et al.* in 2009 [66]. The vertically aligned and patterned CNT forests with high electrical conductivity and a 3D porous network were directly grown on a lithography-patterned Mo/Al conductive substrate. The fabricated prototype microdevice showed a specific capacitance of 428 μF cm^{-2}, about 1000 times higher than that of bare metal electrodes without CNT forests, over 92% charge and discharge efficiency, and robust cycling stability. Recently, the electrodeposition of metal oxides (MnO_2 [67], $Co(OH)_2$ [68]) on vertically aligned and patterned CNTs as positive electrodes for on-chip asymmetric MSCs was developed to increase their power and energy densities because aligned CNTs can provide more accessible interface for charge and discharge. To increase surface area, electrical conductivity and electrochemical performance, Chen *et al.* developed a 3D CNTs/carbon microelectromechanical system (C-MEMS) composites as electrode materials for on-chip supercapacitors. By applying the photolithography and pyrolysis process, 3D C-MEMS architectures were fabricated. After that, catalyst particles were coated on complex 3D structures by electrostatic spray deposition, and thus homogeneous CNTs were catalytically grown onto C-MEMS by CVD [69]. The CNT/C-MEMS composites exhibited 20 times higher specific capacitance than

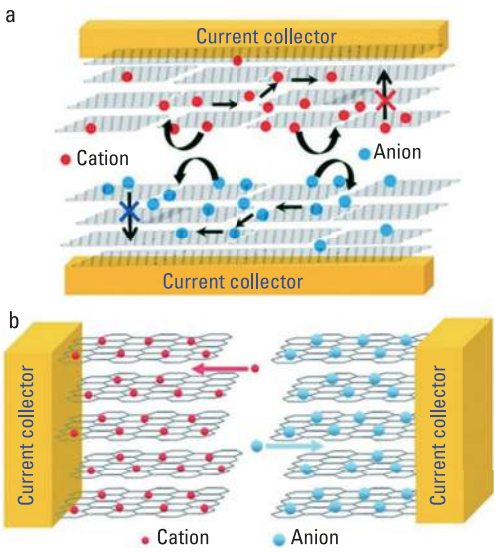

Figure 6. Schematic of supercapacitor devices in (a) stacked geometry and (b) planar geometry. Reprinted with permission from Yoo *et al.* [51]. (Copyright 2010, American Chemical Society.)

C-MEMS. Furthermore, the specific capacitance of CNT/C-MEMS composites increased due to the contribution of oxygen functional groups on the composites induced by oxygen plasma treatment [69]. It was believed that aligned CNT-based MSCs fabricated by MEMS techniques possess promising applications in microsystems, including energy storage, pulse-power supply and on-chip capacitive components.

GRAPHENE-BASED MATERIALS FOR PLANAR INTERDIGITAL MSCs

CVD graphene and reduced graphene oxide

Using 2D atomically thin graphene, new designs for thin-film planar MSCs with desirable performance have become possible, taking full advantage of the atomic layer thicknesses and flat morphology of graphene. Planar MSCs are very favorable for electrolyte ions to interact with the whole surface of the graphene sheets in a short ion diffusion distance, as shown in Fig. 6.

For instance, Yoo *et al.* reported the fabrication of ultrathin planar supercapacitors based on both pristine CVD-grown monolayer graphene and a multilayer reduced graphene oxide (rGO) film [51]. The resulting planar supercapacitors showed a dramatic increase in capacitance compared to conventional sandwich-like supercapacitors. The novel ultrathin planar devices delivered a specific capacitance of ~80 μF cm^{-2} for the CVD-grown monolayer graphene film and up to 394 μF cm^{-2} for the multilayer rGO film.

To explore the full potential of planar supercapacitors, Ajayan's group developed all-graphene-based monolithic MSCs by direct laser reduction and patterning of hydrated graphite oxide (GO) films [11]. Interestingly, it was found that the substantial amount of trapped water in GO enabled it to simultaneously be a good ionic conductor and an electrical insulator, allowing it to serve as both an electrolyte and an electrode separator with ion transport characteristics. To highlight the superiority of the devices, both planar and conventional sandwich-like supercapacitor designs in a number of patterns and shapes (Fig. 7) were directly constructed on one piece of GO paper. The planar supercapacitor with a concentric circular geometry delivered an areal capacitance of ~0.51 mF cm^{-2}, nearly twice that of the sandwich supercapacitor. Furthermore, the MSCs (in a circular geometry) showed good cyclic stability with a ~35% drop in capacitance after 10 000 cycles. The capacitance and energy density of the planar devices were improved with external electrolytes, including an aqueous electrolyte (1.0 M Na_2SO_4) and an organic electrolyte (1.0 M $TEABF_4$). Although the devices obtained gave poor frequency response, large internal resistance (6.5 kΩ) and low rate capability, possibly caused by the long distance between the electrodes of the designed planar geometry, this fabrication technique is promising for large-scale production.

Weng *et al.* reported a simple and scalable approach to manufacture graphene-cellulose paper (GCP) membranes as freestanding and binder-free electrodes for flexible interdigital MSCs (Fig. 8) [70]. The GCP electrode consists of a unique 3D interwoven structure of graphene sheets and cellulose fibers, and has excellent mechanical flexibility. As a consequence, the GCP electrode showed a gravimetric capacitance of 120 F g^{-1} (in graphene weight) and retained >99% capacitance after 5000 cycles. Remarkably, a flexible GCP-based interdigital MSC solidified on a polydimethylsiloxane substrate with a H_2SO_4/PVA gel electrolyte was fabricated (Fig. 8f). The obtained MSC exhibited an areal capacitance of ~7.6 mF cm^{-2}.

Recently, Xu's group developed flexible, ultrathin and all-solid-state graphene-based MSCs, using H_3PO_4/PVA gel electrolyte, through the combination of photolithography with electrophoretic deposition to produce ultrathin rGO interdigital electrodes on a polyethylene terephthalate (PET) substrate (Fig. 9) [71]. Because of the short ion diffusion pathway, the resulting rGO-MSCs exhibited a specific capacitance of 286 F g^{-1}, three times higher

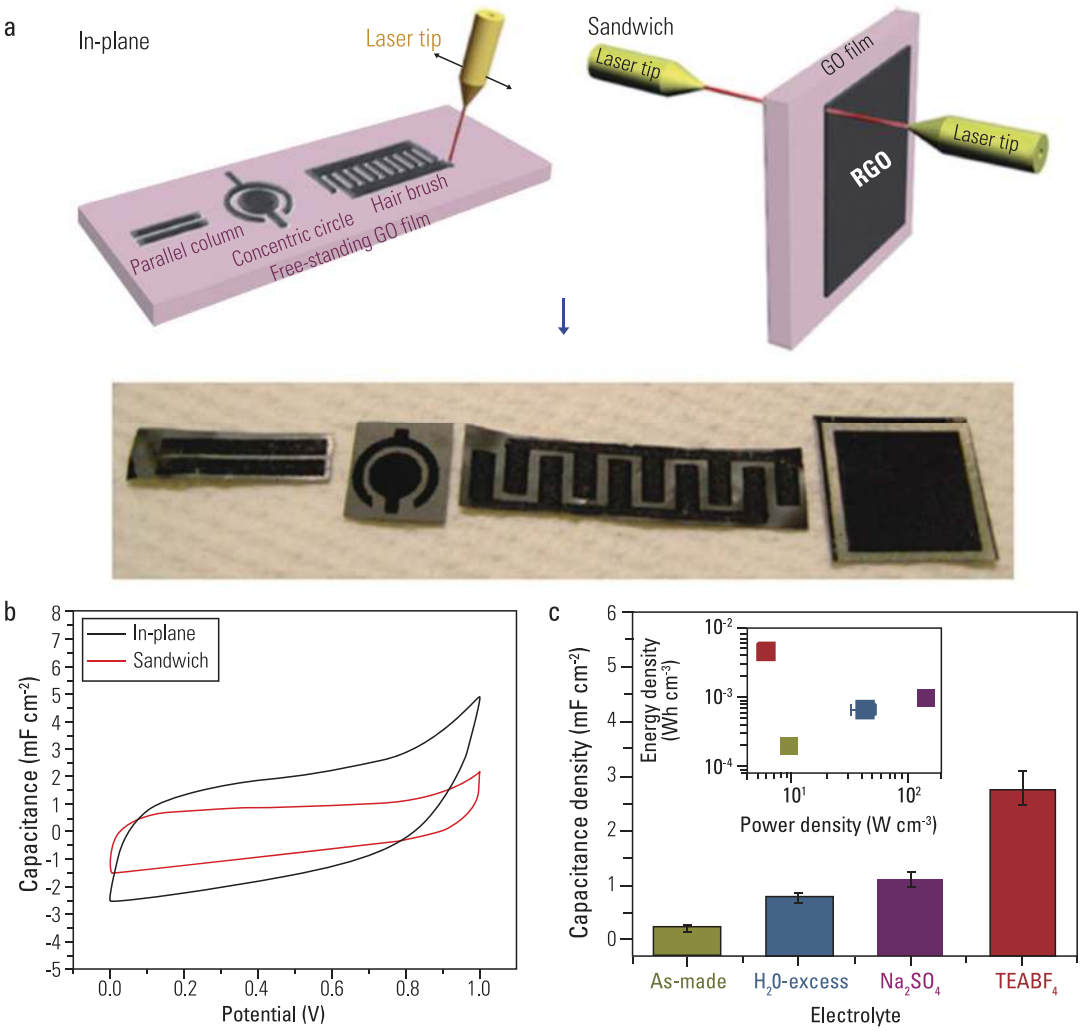

Figure 7. (a) Schematic of laser-patterning of hydrated GO films to fabricate rGO–GO–rGO devices with in-plane and sandwich geometries, and a photograph of the patterned films. (b) CV curves of the in-plane circular and sandwich devices at 40 mV s^{-1}. (c) Comparison of areal capacitance of a sandwich device and MSCs with excess deionized water, 1.0 M Na_2SO_4, and 1.0 M $TEABF_4$ electrolytes. Inset: energy density versus power density of the corresponding devices. Reprinted with permission from Gao *et al.* [11]. (Copyright 2011, Macmillan Publishers Limited.)

than that of conventional rGO-based supercapacitors (~86 F g^{-1}). Significantly, the MSCs can be interconnected in series on one chip to improve the output potential, suggesting the promise for applications in integrated electronics.

Considering the fact that the conventional microfabrication methods involving lithographic techniques or using masks for making micropatterns on substrates are cumbersome for fabricating low-cost micro-devices for widespread applications, El-Kady and Kaner recently reported a scalable fabrication method for graphene-based planar MSCs by direct laser writing on GO films using a standard LightScribe DVD burner [12]. This technique is a simple, low-cost high-throughput lithographic technique that does not require masks, additional processing or complex operations. Fig. 10 shows the fabrication of laser-scribed graphene MSCs (LSG-MSCs). First, a disc with a GO film is inserted into a LightScribe DVD drive, and a computer-designed circuit is written to produce graphene pattern on the GO film by a laser. Second, a copper tape is glued along the edges of the electrodes to improve electrical contact, and the whole interdigital area is covered by a polyimide tape. Finally, an electrolyte is added to obtain a planar LSG-MSC. This process is readily scalable for the efficient fabrication of solid micro-devices that are thin (~7.6 μm) and flexible. For instance, more than 100 microdevices can be quickly produced on a flexible substrate in

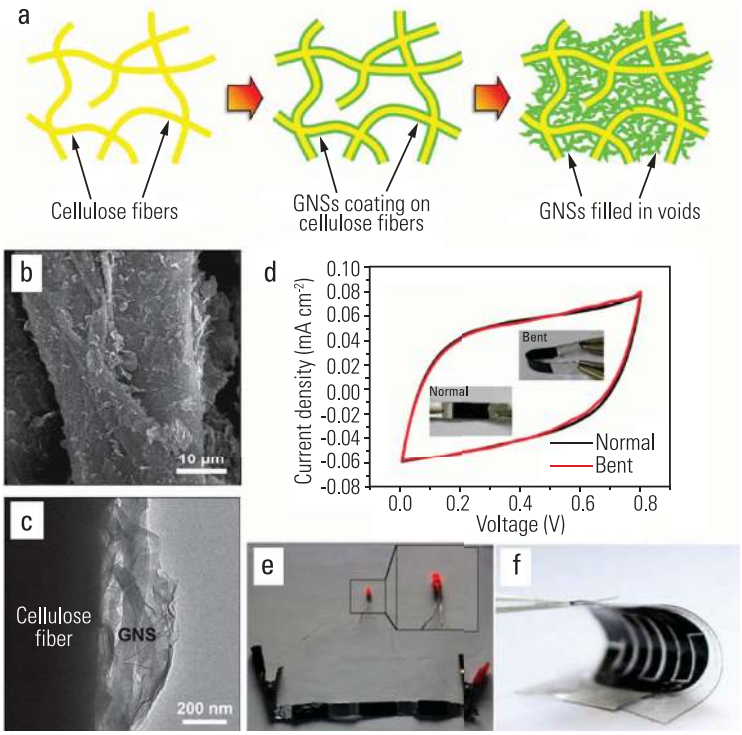

Figure 8. (a) Illustration of the structural evolution of GCP. (b) SEM and (c) TEM images of a cellulose fiber with graphene sheets in a GCP membrane. (d) CV curves of the supercapacitors tested in normal and bent states. (e) A red LED lit by three connected supercapacitors in-series. (f) A flexible GCP-based interdigital MSC. Reprinted with permission from Weng *et al.* [70]. (Copyright 2011, John Wiley & Sons, Inc.)

30 min or less. The MSCs could be built with a hydrogel-polymer electrolyte (H_2SO_4/PVA) or an ionogel electrolyte (1-butyl-3-methylimidazolium bis(trifluoromethylsulfonyl)imide with fumed silica) that respectively allow the operation of the device at a voltage window of 1 V or 2.5 V. The LSG-MSCs (16) have improved charge-storage capacity and rate capability, and offer a resistor–capacitor time constant of 19 ms and a power density of ∼200 W cm^{-3}.

Although the performance of the graphene-based MSCs has been significantly improved by developing thin-film manufacturing technologies and device architectures, their power densities remain far from those of electrolytic capacitors and their energy densities are much lower than those of lithium thin-film batteries. Recently, Wu *et al.* demonstrated a novel class of graphene-based planar interdigital MSCs based on methane plasma reduced graphene (denoted MPG) films micropatterned on arbitrary substrates, both rigid and flexible (Fig. 11) [13]. Due to the high electrical conductivity (∼345 S cm^{-1}) of the MPG films and the planar geometry of the microdevices, the resulting graphene-based MSCs with the H_2SO_4/PVA gel electrolyte deliver an areal capacitance of ∼80.7 μF cm^{-2}, a stack capacitance of ∼17.9 F cm^{-3}, a power density of 495 W cm^{-3} (higher than that of electrolytic capacitors) and an energy density of 2.5 mWh cm^{-3} that is comparable to lithium thin-film batteries, in association with superior cycling stability (∼98.3% capacitance retention after 100 000 cycles at an ultrahigh scan rate of 50 V s^{-1}). These microdevices allow operation at ultrahigh rates up to 1000 V s^{-1}, three orders of magnitude higher than conventional supercapacitors, highlighting the superiority of the planar device geometry over the classical sandwich-like stack geometry for supercapacitors. The fabricated MSCs can also work collaboratively when connected in parallel or in series to meet certain applications that require higher operating currents and voltages in a short time. Furthermore, the devices show an extremely small time constant of ∼0.28 ms that allows them to work in progressively ultrafast charge and discharge conditions [13]. Therefore, the graphene-based MSCs with a planar geometry have great promise for numerous miniaturized or flexible electronic applications.

Graphene quantum dots

In comparison with graphene sheets, graphene quantum dots (GQDs) exhibit novel chemical and physical properties, such as abundant edge defects, good electrical conductivity, chemical stability and easy functionalization, making them promising for building supercapacitor devices [72,73].

Recently, Yan's group reported the use of GQDs as electrode materials for MSCs (GQD-MSCs) [74]. GQD-MSCs with aqueous (0.5 M Na_2SO_4) and ionic liquid ($EMIMBF_4$) electrolytes were fabricated by the electrodeposition of GQDs on interdigital Au microelectrodes (Fig. 12). It was demonstrated that the GQD-MSCs can be operated at ultrahigh scan rates up to 1000 V s^{-1} and achieved fast frequency response with a relaxation time constant of 103.6 μs in an aqueous electrolyte and 53.8 μs in an ionic liquid electrolyte, and excellent cycle performance (∼97.8% capacitance retention after 5000 cycles). The excellent performance of GQD-MSCs is attributed to the advantageous features of GQDs, including a large specific surface area and a large number of surface active sites and accessible edges that provide ample interfaces for easy ion adsorption/desorption, and thus facilitate charge transport through the active layer.

To achieve high-energy and power densities, aqueous asymmetric supercapacitors have been intensively explored by combining a battery-like Faradic electrode (such as metal oxide as the

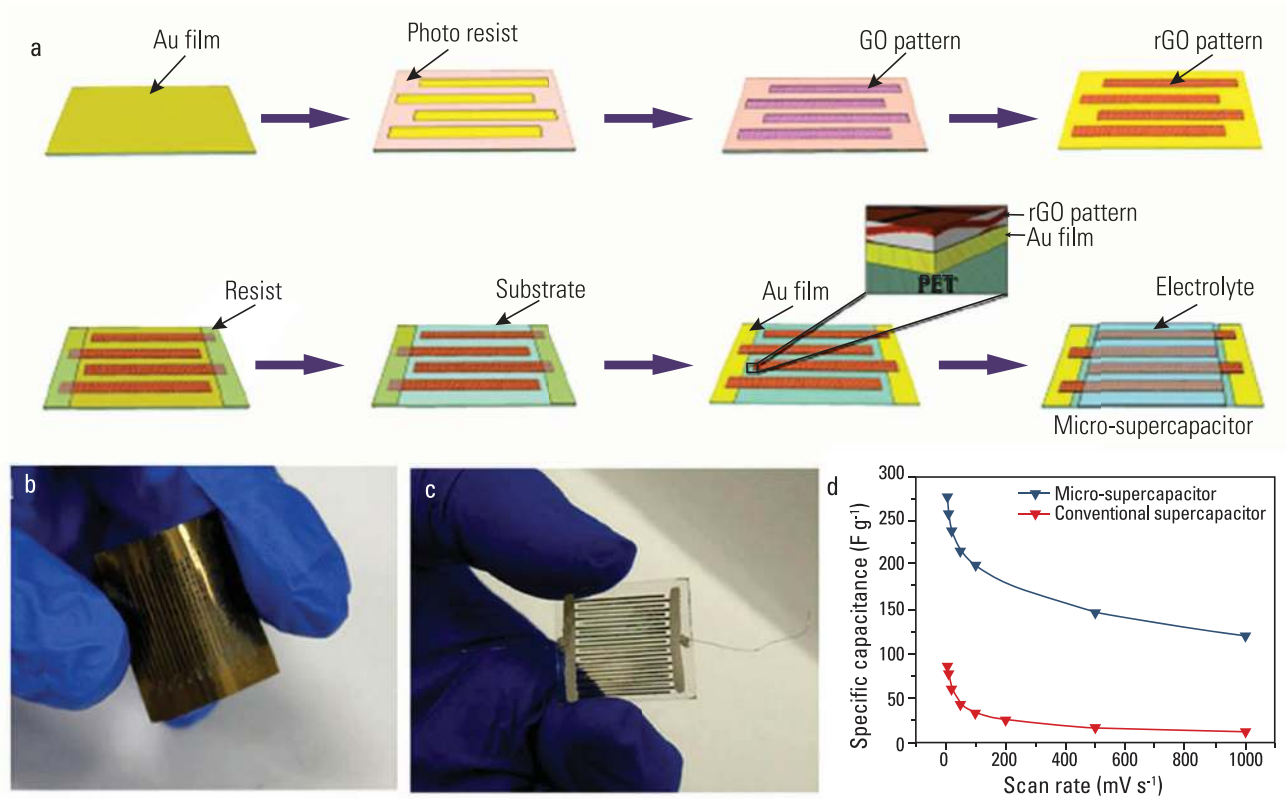

Figure 9. (a) Schematic of fabricating rGO-MSCs on a substrate by combining photolithography with electrophoresis. Optical images of (b) rGO pattern on a PET substrate with a Au film and (c) MSC on a PET substrate. (d) Specific capacitance of the rGO-MSCs and conventional supercapacitors obtained at different scan rates. Reprinted with permission from Niu *et al.* [71]. (Copyright 2013, John Wiley & Sons, Inc.)

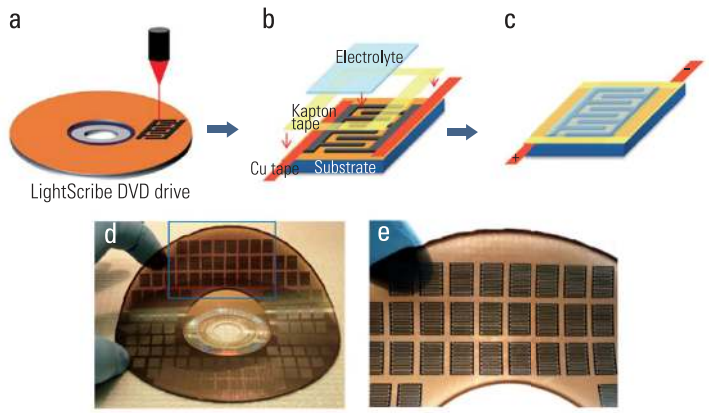

Figure 10. (a–c) Schematic of the fabrication process for LSG-MSCs. (d,e) Direct writing of LSG-MSCs with more than 100 microdevices on a single disc. Reprinted with permission from El-Kady and Kaner [12]. (Copyright 2013, Macmillan Publishers Limited.)

energy source) and a capacitive electrode (such as porous carbon as the power source) to increase operating voltage [75]. Yan's group proposed GQD//MnO_2 asymmetric MSCs, using GQDs as the negative electrode and MnO_2 nanoneedles as the positive electrode in an aqueous electrolyte of 0.5 M Na_2SO_4 [74]. The GQD//MnO_2 asymmetric MSCs were fabricated by two-step electrodeposition. First, GQDs were electrodeposited on one side of the interdigital Au electrodes in a 50 mL DMF solution with 3.0 mg GQDs and 6.0 mg $Mg(NO_3)_2{\cdot}6H_2O$ at a constant voltage of 80 V for 30 min. Second, MnO_2 was electrochemically deposited on the other side of the Au electrodes in a solution of 0.02 M $Mn(NO_3)_2$ and 0.1 M $NaNO_3$ at 1 mA cm^{-2} with the potential window from –1.2 to 1.2 V for 5 min. It was found that both specific capacitance (~1107.4 μF cm^{-2}) and energy density (~0.154 μWh cm^{-2}) of the GQD//MnO_2 asymmetric MSCs are twice those of symmetric GQD-MSCs (~468.1 μF cm^{-2} and 0.074 μWh cm^{-2}) in an aqueous Na_2SO_4 electrolyte. Using a similar approach, this group assembled another all-solid-state asymmetric MSC with a PVA/H_3PO_4 gel electrolyte through the electrodeposition of GQDs as a negative electrode and polyaniline (PANI) nanofiber as a positive electrode on each side of the Au microelectrode [64]. The produced GQD//PANI asymmetric MSCs showed an excellent rate capability of up to 700 V s^{-1}, a short relaxation time constant of 115.9 μs and ~85.6% capacitance retention after 1500 cycles in a solid-state electrolyte.

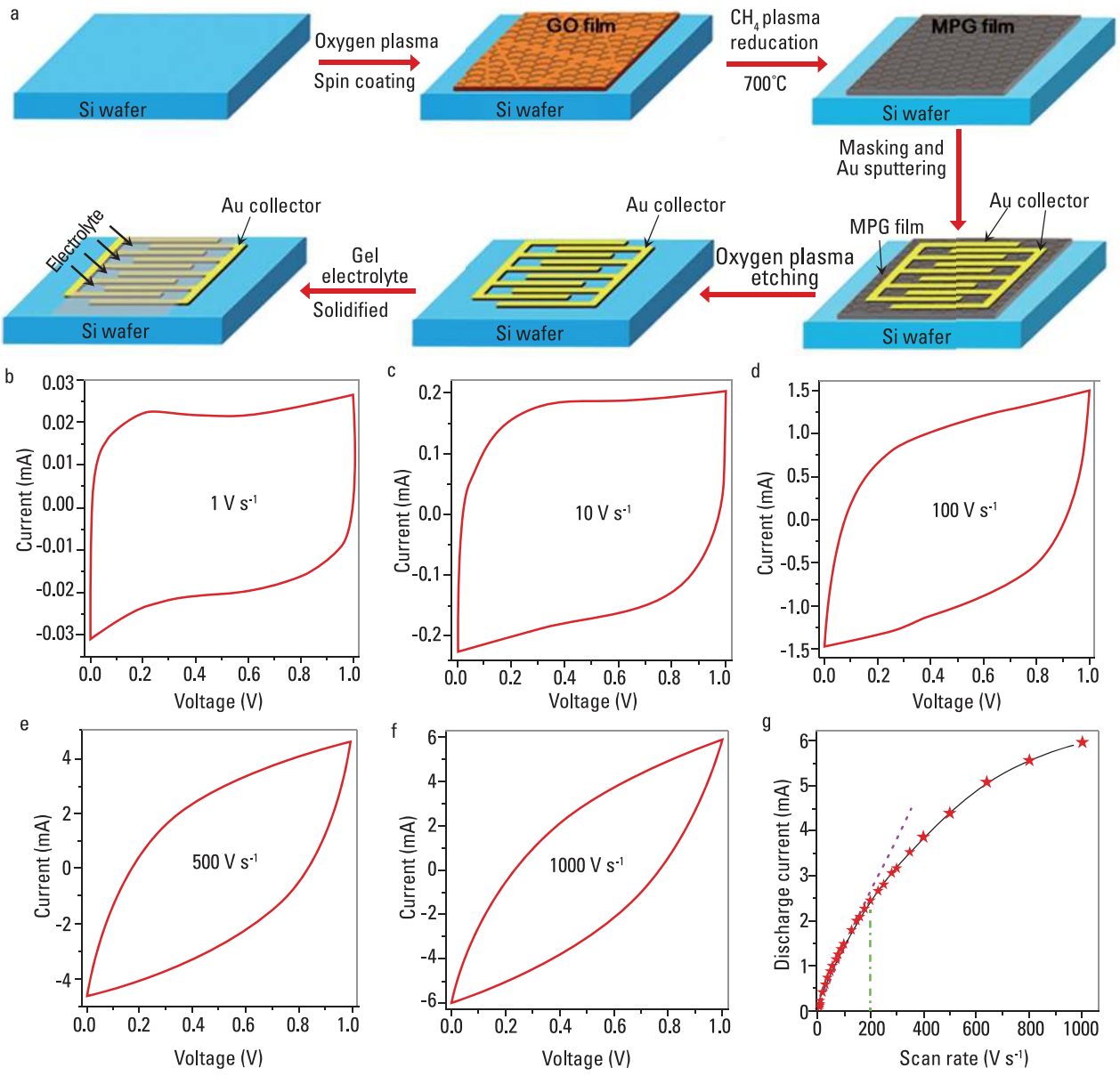

Figure 11. (a) Illustration of the fabrication of all-solid-state interdigital graphene-based MSCs integrated onto a silicon wafer. (b–f) CV curves of the graphene-based MSCs at different scan rates from 1 to 1000 V s^{-1}. (g) A plot of the discharge current as a function of the scan rate. Reprinted with permission from Wu *et al.* [13]. (Copyright 2013, Macmillan Publishers Limited.)

Graphene/carbon nanotube hybrids

As stated above, the planar design can increase the accessibility of ions to the surface of graphene sheets and thus improve the capacitive behavior. Furthermore, one can expect that the capacitance and energy density of planar MSCs can be improved if the electrodes are made by the addition of capacitive spacers, such as CNTs, nanosize metal oxide and electrically conductive polymers between the graphene sheets. The addition of such capacitive spacers not only efficiently prevents the aggregation and restacking of the graphene sheets and increases the accessible surface area for charge storage, but also utilizes the synergetic effect of graphene with the spacers to improve the overall performance of the devices [18].

Wang's group applied electrostatic spray deposition and photolithography lift-off techniques to fabricate interdigital microelectrodes (100 μm width and 50 μm interspace) based on binder-free rGO/ CNT hybrids for MSCs (rGO/CNT-MSCs, Fig. 13) [57]. It was demonstrated that the addition of CNTs between graphene sheets within planar interdigital microelectrodes sufficiently increases the accessibility of electrolyte ions between stacked rGO sheets and improves the energy and power

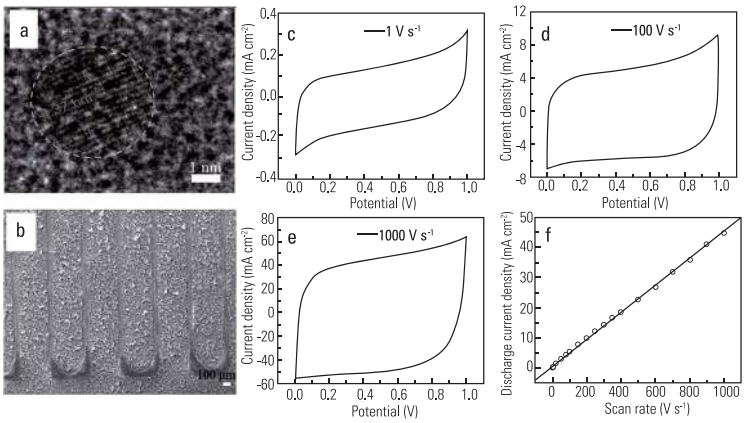

Figure 12. (a) High-resolution TEM image of an individual GQD. (b) Top-view SEM image of Au interdigital electrodes deposited with GQDs. (c–e) CV curves of GQD-MSCs in 0.5 M Na_2SO_4 at (c) 1, (d) 100 and (e) 1000 V s^{-1}, respectively. (f) The charge current density of GQD-MSCs as a function of scan rate. Reprinted with permission from Liu *et al.* [74]. (Copyright 2013, John Wiley & Sons, Inc.)

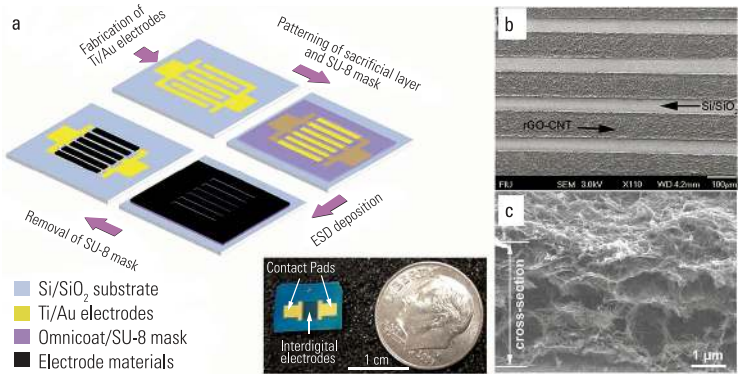

Figure 13. (a) Schematic of the fabrication of rGO/CNT-MSCs (inset: digital photograph of one MSC). (b) Top-view and (c) cross-section SEM images of rGO/CNT-based interdigital microelectrodes. Reprinted with permission from Beidaghi and Wang [57]. (Copyright 2012, John Wiley & Sons, Inc.)

densities. The rGO/CNT-MSCs showed a specific areal capacitance of ∼6.1 mF cm^{-2} at a low scan rate of 0.01 V s^{-1} and ∼2.8 mF cm^{-2} (stack capacitance of ∼3.1 F cm^{-3}) at a high scan rate of 50 V s^{-1}. This micro-device had a low time constant of 4.8 ms, an energy density of ∼0.68 mWh cm^{-3} and a power density of ∼77 W cm^{-3}, all of which are much higher than those of MSCs based on pure rGO or CNTs [57]. The improved performance of rGO/CNT-MSCs is attributed to the synergetic combination of the advantages of graphene, CNTs, electrolyte-accessible and binder-free microelectrodes, and the interdigital planar geometry in one device.

To achieve a high-energy density while maintaining satisfactory alternating current (ac) line filtering performance in a single device, Lin *et al.* fabricated 3D graphene/CNT carpet (G/CNTC)-based MSCs (G/CNTC-MSCs) on nickel electrodes (Fig. 14) [76]. The G/CNTC-MSCs exhibited an impedance phase angle of −81.5° at a frequency of 120 Hz, close to that of commercial aluminum electrolytic capacitors (AECs, 83.9°) for ac line filtering applications. As a consequence, G/CNTC-MSCs delivered a high volumetric energy density of 2.42 mWh cm^{-3} in an ionic liquid (BMIM-BF_4), an ultrahigh rate capability of ∼400 V s^{-1} and a high power density of 115 W cm^{-3} in an aqueous electrolyte (1M Na_2SO_4). The excellent electrochemical performance of the G/CNTC-MSCs is likely due to the seamless nanotube/graphene junctions at the interface of the different carbon allotropic forms.

Graphene/metal oxide hybrids

To improve the capacitive performance of planar MSCs, Peng and co-workers reported novel planar MSCs based on a hybrid nanostructure of ultrathin MnO_2/graphene sheets (denoted MnO_2/G-MSCs), using a gel electrolyte of PVA/H_3PO_4 (Fig. 15) [77]. The fabrication procedure of flexible planar MnO_2/G-MSCs includes the preparation of a MnO_2/G hybrid film by the vacuum filtration of a MnO_2/graphene solution, transferring a thin hybrid film onto a PET substrate, scraping the thin film to obtain slim strips as working electrodes, thermal evaporation of Au current collectors on both sides of the working electrodes, coating gel electrolyte on the parallel interspaces between the electrodes and finally constructing a planar MnO_2/G-MSC [77]. The hybrid of ultrathin MnO_2 sheets and graphene sheets not only offers sufficient electrochemically active surface for fast absorption/desorption of electrolyte ions, but also possesses additional interfaces at the hybridized interlayer areas to accelerate charge transport during charge/discharge process. The MnO_2/G-MSCs obtained showed improved electrochemical performance compared with graphene-based MSCs, including a high specific capacitance of ∼267 F g^{-1} at 0.2 A g^{-1} and 208 F g^{-1} at 10 A g^{-1}, good rate capability and exceptional cycling stability (∼92% capacitance retention after 7000 cycles). Moreover, the MnO_2/G-MSCs exhibited superior flexibility and cyclability, yielding capacitance retention over 90% after 1000 folding/unfolding cycles.

OUTLOOK AND PROSPECTIVES

We have summarized the recent development of graphene-based materials for on-chip planar interdigital MSCs, which combine the advantages of both graphene and a planar geometry. In

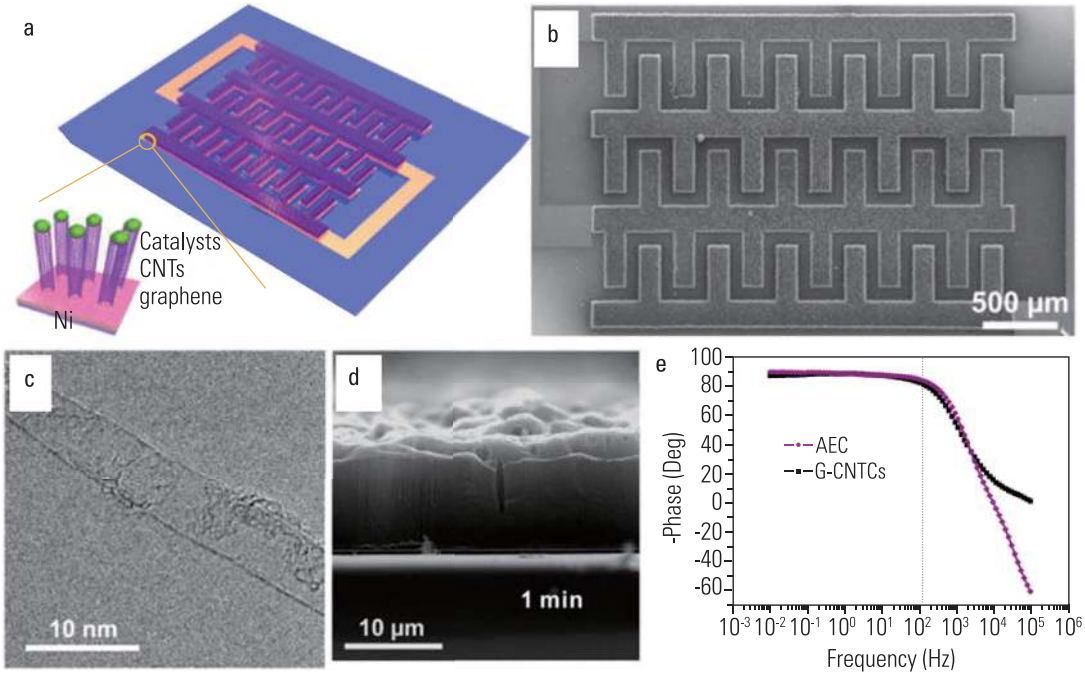

Figure 14. (a) Schematic of the structure of G/CNTC-MSCs. Inset: enlarged scheme of a Ni-G-CNTC pillar structure. (b) SEM image of the G/CNTCs-MSCs fabricated. (c) TEM image of a single-wall CNT. (d) SEM image of CNTCs grown for 1 min. (e) Impedance phase angle versus frequency of G/CNTC-MSCs and AECs. Reprinted with permission from Lin *et al.* [76]. (Copyright 2013, American Chemical Society.)

particular, the 2D ultrathin structure, excellent electrical conductivity, high surface area ($\sim$2620 $m^2 g^{-1}$) and high theoretical capacitance ($\sim$550 $F g^{-1}$) of graphene enable it to be a very promising electrode material for planar MSCs that can greatly improve the charge/discharge performance, promote the rapid diffusion of ions into or out of the internal structure of the electrodes using short pathways and increase the accessibility of ions to the surface of all the parallel graphene sheets on substrates [51]. Furthermore, the planar device geometry provides two major merits compared with conventional supercapacitor devices with a stacking geometry of thin-film electrodes. One is that both positive and negative electrodes are in one plane, which allows for elaborate integration with an electronic device chip [12]. Another advantage is the improved performance of planar MSCs with interdigital electrodes compared to that of conventional devices [13]. As a result, the latest advancements of graphene-based interdigital MSCs based on graphene sheets, GQDs and their hybrids have demonstrated outstanding electrochemical performance with a large scan rate, fast frequency response, long-term cycling stability, and ultrahigh power and energy densities, which are superior to the classical sandwich-type supercapacitors and any other previously reported MSCs with other carbons as electrode materials [12,13].

Further development of graphene-based MSCs will consider the integration of the following crucial aspects into one device. First, the designed fabrication of nanostructured electroactive materials (graphene and graphene-based hybrids) is crucial for the fundamental improvement of MSCs [3]. In fact, the research and development of graphene-based MSCs are still in very early fundamental stage and many issues remain to be solved. The ability to tune the morphology and microstructure of graphene sheets on films is a very important feature to increase the performance of the resulting MSCs. In principle, this can be achieved through an accurate modification of special parameters of graphene films with a narrow pore size distribution, large specific surface area, high-concentration heteroatom (N, B) doping, high electrical conductivity and the introduction of other nanostructural electroactive species. In fact, understanding the complex relationship between the structure and capacitive performance of graphene materials is absolutely necessary to improve the design of high-performance graphene-based MSCs. Considering the fact that the 2D nature of graphene in MSCs can significantly enhance the ability of electrolyte ions to interact

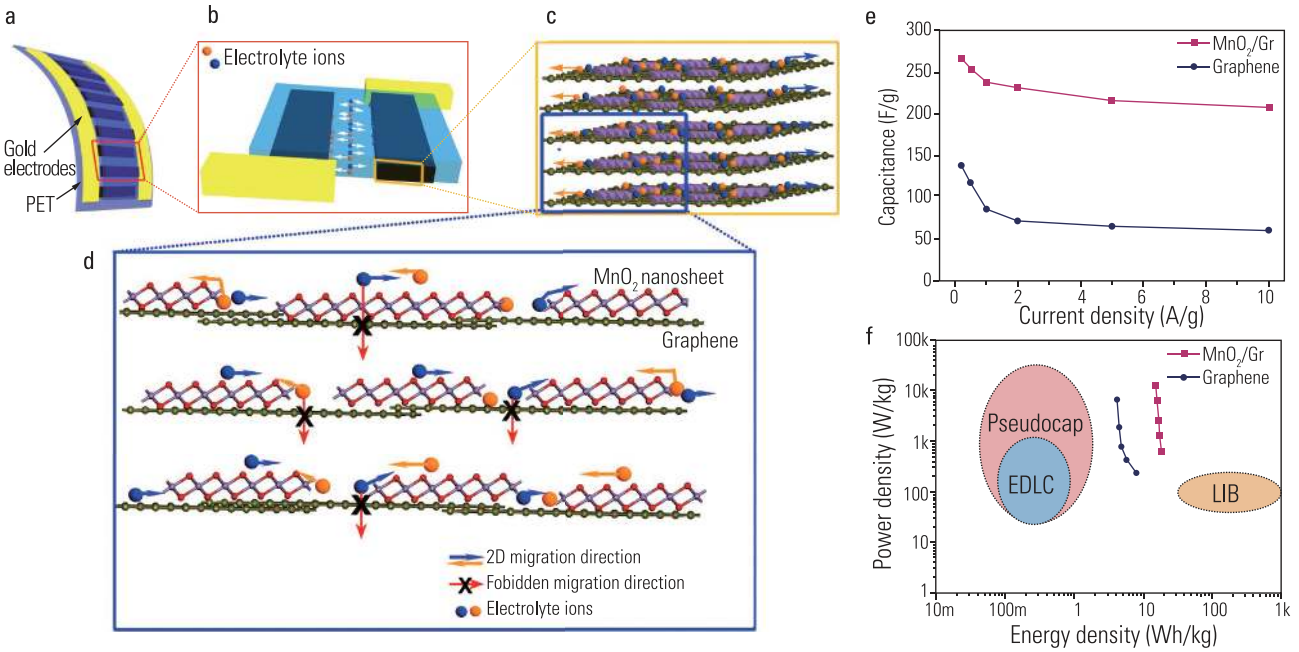

Figure 15. (a) Schematic of MnO_2/G-MSCs. (b) The planar MSC unit. (c) The hybrid thin film was stacked by the layers of δ-MnO_2 sheets and graphene sheets. (d) Schematic description of the ion transport favored within the δ-MnO_2/G hybrid. (e) Capacitance comparison of MnO_2/G-MSCs (MnO_2/Gr) and graphene MSCs. (f) A Ragone plot of the MnO_2/G-MSCs. Reprinted with permission from Peng *et al.* [77]. (Copyright 2013, American Chemical Society.)

with all the graphene sheets in the horizontal direction, other graphene analogues, such as inorganic oxide and sulfide sheets (such as MnO_2, RuO_2, TiO_2, Co_3O_4, VS_2), can also serve as promising electrode materials for novel MSCs.

Second, developing new, simple, low-cost thin-film manufacturing technologies that can produce uniform, conductive, large-area films on arbitrary substrates is another key issue to obtain high-performance MSCs. The strategies developed for thin-film production include spin coating, casting, painting, vacuum filtration, electrochemical polymerization and layer-by-layer assembly, some of which are quite effective in improving the performance of microdevices. To address this goal, two key aspects should be considered. One is the solution processibility of graphene-based materials compatible with the substrate surface, which is indispensable for improving the device performance. Another is the scalability of thin-film techniques that should be efficient for the production of continuous large-area thin films. In this regard, inkjet printing [56,78] or screen printing [79] technology may hold great promise for the deposition of nanocarbons, polymers, oxides and metals for MSCs. These techniques are inexpensive, rapid and capable of mass production for the large-scale fabrication of thin-film-based MSCs on a broad variety of substrates, such as silicon wafers, paper, plastics, etc., but there has, as yet, been no systematic study of their use for producing graphene-based materials for MSCs. It is expected that these techniques should be both useful and readily applicable to the thin-film processing of a wide range of materials for large-area devices which can be easily incorporated into electronics.

Last but not least, further optimization of full device architectures is a long-term challenging issue. Current research attempts have made great progress in the configuration of planar interdigital MSCs with improved energy and power densities, but it is still necessary to optimize the main geometric parameters including the interspace, width, length and number of fingers. An appropriate geometric adjustment of these parameters for increasing the active area by increasing the number (width, length) of fingers or reducing the interspace between adjacent fingers can efficiently decrease the device resistance and thus increase the energy and power densities of MSCs. Alternatively, developing 3D graphene-based interdigital MSCs by lithographical microfabrication techniques can increase the amount of active material loaded per area while fast ion diffusion is unaffected, leading to an improvement of the output power and energy [7,58,60,80]. Regarding the practical applications, the connection of two or more MSCs in parallel and/or series within one MSC pack on a large-area substrate is expected to be a promising strategy to meet the urgent requirements for portable electronics and other on-chip uses [13].

We anticipate that further improvement in the performance of graphene-based MSCs can be achieved through the reasonable optimization of the composition of the active electrode materials, thin-film manufacturing techniques, interfacial integrity of the main components (electrode, separator, electrolyte and substrate) and micro-electrode design as well as the selection of the electrolytes. We believe that the current advancement of graphene-based MSCs should address the urgent need for micro-scale energy storage. Graphene-based MSCs promise ultrahigh energy and power micro-electrochemical energy-storage devices that are able to offer enough energy and satisfy the peak power required for a great number of applications in miniaturized electronic devices.

FUNDING

This work was financially supported by National Natural Science Foundation of China (51172240, 51290273, 50921004 and 50972147), Ministry of Science and Technology of China (2012AA030303) and Chinese Academy of Sciences (KGZD-EW-303–1), and ERC grants on 2DMATER, DFG Priority Program SPP 1459, and EC under Graphene Flagship (CNECT-ICT-604391).

REFERENCES

1. Simon, P and Gogotsi, Y. Materials for electrochemical capacitors. *Nat Mater* 2008; **7**: 845–54.
2. Miller, JR and Simon, P. Electrochemical capacitors for energy management. *Science* 2008; **321**: 651–2.
3. Arico, AS, Bruce, P and Scrosati, B *et al.* Nanostructured materials for advanced energy conversion and storage devices. *Nat Mater* 2005; **4**: 366–77.
4. Liu, C, Li, F and Ma, LP *et al.* Advanced materials for energy storage. *Adv Mater* 2010; **22**: E28–E62.
5. Wang, DW, Li, F and Liu, M *et al.* 3D aperiodic hierarchical porous graphitic carbon material for high-rate electrochemical capacitive energy storage. *Angew Chem Int Edit* 2008; **47**: 373–6.
6. Frackowiak, E and Beguin, F. Carbon materials for the electrochemical storage of energy in capacitors. *Carbon* 2001; **39**: 937–50.
7. Rolison, DR, Long, RW and Lytle, JC *et al.* Multifunctional 3D nanoarchitectures for energy storage and conversion. *Chem Soc Rev* 2009; **38**: 226–52.
8. Arthur, TS, Bates, DJ and Cirigliano, N *et al.* Three-dimensional electrodes and battery architectures. *MRS Bull* 2011; **36**: 523–31.
9. Chmiola, J, Largeot, C and Taberna, PL *et al.* Monolithic carbide-derived carbon films for micro-supercapacitors. *Science* 2010; **328**: 480–3.
10. Pech, D, Brunet, M and Durou, H *et al.* Ultrahigh-power micrometre-sized supercapacitors based on onion-like carbon. *Nat Nanotechnol* 2010; **5**: 651–4.
11. Gao, W, Singh, N and Song, L *et al.* Direct laser writing of micro-supercapacitors on hydrated graphite oxide films. *Nat Nanotechnol* 2011; **6**: 496–500.
12. El-Kady, MF and Kaner, RB. Scalable fabrication of high-power graphene micro-supercapacitors for flexible and on-chip energy storage. *Nat Commun* 2013; **4**: 1475.
13. Wu, ZS, Parvez, K and Feng, XL *et al.* Graphene-based in-plane micro-supercapacitors with ultrahigh power and energy densities. *Nat Commun* 2013; **4**: 2487.
14. Stoller, MD, Park, SJ and Zhu, YW *et al.* Graphene-based ultracapacitors. *Nano Lett* 2008; **8**: 3498–502.
15. Hashmi, SA. Supercapacitor: an emerging power source. *Natl Acad Sci Lett* 2004; **27**: 27–46.
16. Kotz, R and Carlen, M. Principles and applications of electrochemical capacitors. *Electrochim Acta* 2000; **45**: 2483–98.
17. Zhai, Y, Dou, Y and Zhao, D *et al.* Carbon materials for chemical capacitive energy storage. *Adv Mater* 2011; **23**: 4828–50.
18. Wu, ZS, Zhou, GM and Yin, LC *et al.* Graphene/metal oxide composite electrode materials for energy storage. *Nano Energy* 2012; **1**: 107–31.
19. Wu, ZS, Winter, A and Chen, L *et al.* Three-dimensional nitrogen and boron co-doped graphene for high-performance all-solid-state supercapacitors. *Adv Mater* 2012; **24**: 5130–5.
20. Wu, ZS, Sun, Y and Tan, YZ *et al.* Three-dimensional graphene-based macro- and mesoporous frameworks for high-performance electrochemical capacitive energy storage. *J Am Chem Soc* 2012; **134**: 19532–5.
21. Weng, Z, Li, F and Wang, DW *et al.* Controlled electrochemical charge injection to maximize the energy density of supercapacitors. *Angew Chem Int Edit* 2013; **52**: 3722–5.
22. Novoselov, KS, Geim, AK and Morozov, SV *et al.* Electric field effect in atomically thin carbon films. *Science* 2004; **306**: 666–9.
23. Berger, C, Song, ZM and Li, TB *et al.* Ultrathin epitaxial graphite: 2D electron gas properties and a route toward graphene-based nanoelectronics. *J Phys Chem B* 2004; **108**: 19912–6.
24. Berger, C, Song, ZM and Li, XB *et al.* Electronic confinement and coherence in patterned epitaxial graphene. *Science* 2006; **312**: 1191–6.
25. Park, S and Ruoff, RS. Chemical methods for the production of graphenes. *Nat Nanotechnol* 2009; **4**: 217–24.
26. Coleman, JN. Liquid-phase exfoliation of nanotubes and graphene. *Adv Funct Mater* 2009; **19**: 3680–95.
27. Wu, ZS, Ren, W and Gao, L *et al.* Synthesis of high-quality graphene with a pre-determined number of layers. *Carbon* 2009; **47**: 493–9.
28. Wu, ZS, Ren, WC and Gao, LB *et al.* Efficient synthesis of graphene nanoribbons sonochemically cut from graphene sheets. *Nano Res* 2010; **3**: 16–22.
29. Wu, ZS, Ren, WC and Gao, LB *et al.* Synthesis of graphene sheets with high electrical conductivity and good thermal stability by hydrogen arc discharge exfoliation. *ACS Nano* 2009; **3**: 411–7.
30. Li, XS, Cai, WW and An, JH *et al.* Large-area synthesis of high-quality and uniform graphene films on copper foils. *Science* 2009; **324**: 1312–4.

31. Reina, A, Jia, XT and Ho, J *et al.* Large area, few-layer graphene films on arbitrary substrates by chemical vapor deposition. *Nano Lett* 2009; **9**: 30–5.
32. Chen, ZP, Ren, WC and Gao, LB *et al.* Three-dimensional flexible and conductive interconnected graphene networks grown by chemical vapour deposition. *Nat Mater* 2011; **10**: 424–8.
33. Zhi, LJ and Müllen, K. A bottom-up approach from molecular nanographenes to unconventional carbon materials. *J Mater Chem* 2008; **18**: 1472–84.
34. Yang, XY, Dou, X and Rouhanipour, A *et al.* Two-dimensional graphene nanoribbons. *J Am Chem Soc* 2008; **130**: 4216–7.
35. Parvez, K, Li, RJ and Puniredd, SR *et al.* Electrochemically exfoliated graphene as solution-processable, highly conductive electrodes for organic electronics. *ACS Nano* 2013; **7**: 3598–606.
36. Pang, SP, Hernandez, Y and Feng, XL *et al.* Graphene as transparent electrode material for organic electronics. *Adv Mater* 2011; **23**: 2779–95.
37. Stankovich, S, Dikin, DA and Dommett, GHB *et al.* Graphene-based composite materials. *Nature* 2006; **442**: 282–6.
38. Wang, X, Zhi, LJ and Müllen, K. Transparent, conductive graphene electrodes for dye-sensitized solar cells. *Nano Lett* 2008; **8**: 323–7.
39. Wu, ZS, Ren, W and Wen, L *et al.* Graphene anchored with Co_3O_4 nanoparticles as anode of lithium ion batteries with enhanced reversible capacity and cyclic performance. *ACS Nano* 2010; **4**: 3187–94.
40. Wu, ZS, Ren, WC and Xu, L *et al.* Doped graphene sheets as anode materials with superhigh rate and large capacity for lithium ion batteries. *ACS Nano* 2011; **5**: 5463–71.
41. Wu, ZS, Xue, LL and Ren, WC *et al.* A LiF nanoparticle-modified graphene electrode for high-power and high-energy lithium ion batteries. *Adv Funct Mater* 2012; **22**: 3290–7.
42. Wu, ZS, Wang, DW and Ren, W *et al.* Anchoring hydrous RuO_2 on graphene sheets for high-performance electrochemical capacitors. *Adv Funct Mater* 2010; **20**: 3595–602.
43. Yavari, F, Chen, ZP and Thomas, AV *et al.* High sensitivity gas detection using a macroscopic three-dimensional graphene foam network. *Sci Rep* 2011; **1**: 166.
44. Wu, ZS, Pei, S and Ren, W *et al.* Field emission of single-layer graphene films prepared by electrophoretic deposition. *Adv Mater* 2009; **21**: 1756–60.
45. Wu, ZS, Yang, SB and Sun, Y *et al.* 3D nitrogen-doped graphene aerogel-supported Fe_3O_4 nanoparticles as efficient eletrocatalysts for the oxygen reduction reaction. *J Am Chem Soc* 2012; **134**: 9082–5.
46. Xia, JL, Chen, F and Li, JH *et al.* Measurement of the quantum capacitance of graphene. *Nat Nanotechnol* 2009; **4**: 505–9.
47. Miller, JR, Outlaw, RA and Holloway, BC. Graphene double-layer capacitor with ac line-filtering performance. *Science* 2010; **329**: 1637–9.
48. El-Kady, MF, Strong, V and Dubin, S *et al.* Laser scribing of high-performance and flexible graphene-based electrochemical capacitors. *Science* 2012; **335**: 1326–30.
49. Liu, CG, Yu, ZN and Neff, D *et al.* Graphene-based supercapacitor with an ultrahigh energy density. *Nano Lett* 2010; **10**: 4863–8.
50. Zhu, YW, Murali, S and Stoller, MD *et al.* Carbon-based supercapacitors produced by activation of graphene. *Science* 2011; **332**: 1537–41.
51. Yoo, JJ, Balakrishnan, K and Huang, JS *et al.* Ultrathin planar graphene supercapacitors. *Nano Lett* 2011; **11**: 1423–7.
52. Pech, D, Brunet, M and Dinh, TM *et al.* Influence of the configuration in planar interdigitated electrochemical micro-capacitors. *J Power Sources* 2013; **230**: 230–5.
53. Sung, JH, Kim, SJ and Lee, KH. Fabrication of microcapacitors using conducting polymer microelectrodes. *J Power Sources* 2003; **124**: 343–50.
54. Sung, JH, Kim, S and Lee, KH. Fabrication of all-solid-state electrochemical microcapacitors. *J Power Sources* 2004; **133**: 312–9.
55. Sung, JH, Kim, SJ and Jeong, SH *et al.* Flexible micro-supercapacitors. *J Power Sources* 2006; **162**: 1467–70.
56. Pech, D, Brunet, M and Taberna, PL *et al.* Elaboration of a microstructured inkjet-printed carbon electrochemical capacitor. *J Power Sources* 2010; **195**: 1266–9.
57. Beidaghi, M and Wang, CL. Micro-supercapacitors based on interdigital electrodes of reduced graphene oxide and carbon nanotube composites with ultra high power handling performance. *Adv Funct Mater* 2012; **22**: 4501–10.
58. Beidaghi, M and Wang, CL. Micro-supercapacitors based on three dimensional interdigital polypyrrole/C-MEMS electrodes. *Electrochim Acta* 2011; **56**: 9508–14.
59. Durou, H, Pech, D and Colin, D *et al.* Wafer-level fabrication process for fully encapsulated micro-supercapacitors with high specific energy. *Microsyst Technol* 2012; **18**: 467–73.
60. Shen, CW, Wang, XH and Zhang, WF *et al.* A high-performance three-dimensional micro supercapacitor based on self-supporting composite materials. *J Power Sources* 2011; **196**: 10465–71.
61. Makino, S, Yamauchi, Y and Sugimoto, W. Synthesis of electro-deposited ordered mesoporous RuO_x using lyotropic liquid crystal and application toward micro-supercapacitors. *J Power Sources* 2013; **227**: 153–60.
62. Xue, MQ, Xie, Z and Zhang, LS *et al.* Microfluidic etching for fabrication of flexible and all-solid-state micro supercapacitor based on MnO_2 nanoparticles. *Nanoscale* 2011; **3**: 2703–8.
63. Feng, J, Sun, X and Wu, CZ *et al.* Metallic few-layered VS_2 ultrathin nanosheets: high two-dimensional conductivity for in-plane supercapacitors. *J Am Chem Soc* 2011; **133**: 17832–8.
64. Liu, WW, Yan, XB and Chen, JT *et al.* Novel and high-performance asymmetric micro-supercapacitors based on graphene quantum dots and polyaniline nanofibers. *Nanoscale* 2013; **5**: 6053–62.
65. Huang, P, Heon, M and Pech, D *et al.* Micro-supercapacitors from carbide derived carbon (CDC) films on silicon chips. *J Power Sources* 2013; **225**: 240–4.
66. Jiang, YQ, Zhou, Q and Lin, L. Planar MEMS supercapacitor using carbon nanotube forests. *IEEE 22nd International Conference on Micro Electro Mechanical Systems,*. 2009; 587–90.
67. Liu, CC, Tsai, DS and Chung, WH *et al.* Electrochemical micro-capacitors of patterned electrodes loaded with manganese oxide and carbon nanotubes. *J Power Sources* 2011; **196**: 5761–8.
68. Chen, CH, Tsai, DS and Chung, WH *et al.* Electrochemical capacitors of miniature size with patterned carbon nanotubes and cobalt hydroxide. *J Power Sources* 2012; **205**: 510–5.
69. Chen, W, Beidaghi, M and Penmatsa, V *et al.* Integration of carbon nanotubes to C-MEMS for on-chip supercapacitors. *IEEE T Nanotechnol* 2010; **9**: 734–40.
70. Weng, Z, Su, Y and Wang, DW *et al.* Graphene-cellulose paper flexible supercapacitors. *Adv Energy Mater* 2011; **1**: 917–22.
71. Niu, ZQ, Zhang, L and Liu, LL *et al.* All-solid-state flexible ultrathin micro-supercapacitors based on graphene. *Adv Mater* 2013; **25**: 4035–42.
72. Shinde, DB and Pillai, VK. Electrochemical resolution of multiple redox events for graphene quantum dots. *Angew Chem Int Edit* 2013; **52**: 2482–5.
73. Li, Y, Hu, Y and Zhao, Y *et al.* An electrochemical avenue to green-luminescent graphene quantum dots as potential electron-acceptors for photovoltaics. *Adv Mater* 2011; **23**: 776–80.
74. Liu, WW, Feng, YQ and Yan, XB *et al.* Superior micro-supercapacitors based on graphene quantum dots. *Adv Funct Mater* 2013; **23**: 4111–22.

75. Wu, ZS, Ren, WC and Wang, DW *et al.* High-energy MnO_2 nanowire/graphene and graphene asymmetric electrochemical capacitors. *ACS Nano* 2010; **4**: 5835–42.
76. Lin, J, Zhang, CG and Yan, Z *et al.* 3-dimensional graphene carbon nanotube carpet-based microsupercapacitors with high electrochemical performance. *Nano Lett* 2013; **13**: 72–8.
77. Peng, LL, Peng, X and Liu, BR *et al.* Ultrathin two-dimensional MnO_2/graphene hybrid nanostructures for high-performance, flexible planar supercapacitors. *Nano Lett* 2013; **13**: 2151–7.
78. Chen, PC, Chen, HT and Qiu, J *et al.* Inkjet printing of single-walled carbon nanotube/RuO_2 nanowire supercapacitors on cloth fabrics and flexible substrates. *Nano Res* 2010; **3**: 594–603.
79. Xu, YF, Schwab, MG and Strudwick, AJ *et al.* Screen-printable thin film supercapacitor device utilizing graphene/polyaniline inks. *Adv Energy Mater* 2013; **3**: 1035–40.
80. Pikul, JH, Zhang, HG and Cho, J *et al.* High-power lithium ion microbatteries from interdigitated three-dimensional bicontinuous nanoporous electrodes. *Nat Commun* 2013; **4**: 1732.